

Quantum Efficiency of Intermediate-Band Solar Cells Based on Non-Compensated n-p Codoped TiO_2

Fengcheng Wu,¹ Haiping Lan,¹ Zhenyu Zhang,^{1,2} and Ping Cui^{1, a)}

¹*ICQD, Hefei National Laboratory for Physical Sciences at the Microscale, University of Science and Technology of China, Hefei, 230026, People's Republic of China*

²*Department of Physics and Astronomy, University of Tennessee, Knoxville, Tennessee 37996, USA*

(Dated: 21 June 2011)

We explore theoretically the optimal quantum efficiency of intermediate-band solar cells (IBSCs) based on non-compensated n-p codoped TiO_2 under two different design schemes. The first preserves the ideal condition that no electrical current be extracted from the intermediate band (IB). The corresponding maximum quantum efficiency for the codoped TiO_2 can reach 52.7%. In the second scheme, current is also extracted from the IB, resulting in a further enhancement in the maximum efficiency to 56.7%. Our findings also relax the stringent requirement that the IB location be close to the optimum value, making it more feasible to realize IBSCs with high quantum efficiencies.

In recent years, several innovative concepts have been proposed for developing third-generation photovoltaic solar cells of high efficiency. Multi-junction cells maintain the world record on conversion efficiency, exceeding 40%¹. However, their commercial production is severely limited by the complexity of the device fabrication process. Intermediate-band solar cells (IBSCs)² provide an intuitive approach to significantly increase photovoltaic conversion efficiency in a single-junction solar cell device. A properly located intermediate band (IB) in the intrinsic bandgap serves as a “stepping stone” in allowing photons with energies below the bandgap to excite electrons from the valence band (VB) to the conduction band (CB) via a two-step process. Through these additional excitation channels, the lower-energy photons are able to contribute to the photocurrent as well, resulting in a maximum efficiency of 63.2%, substantially higher than the Shockley-Queisser limit of 40.7% for single bandgap solar cells³. Since its conception, much effort has been devoted to exploring different aspects of IBSCs^{4–11}, and several key ingredients of the concept have been convincingly established^{4–6}. However, so far high-efficiency, IBSCs are still yet to be developed⁷; one standing challenge is how to controllably build IBs in the intrinsic bandgaps of candidate materials.

Recently, a new scheme, termed as non-compensated n-p codoping, has been proposed to create one or more tunable IBs in wide bandgap oxide semiconductors, as demonstrated for TiO_2 ¹². In this scheme, both the thermodynamic and kinetic solubilities of the dopants are enhanced by the Coulomb attraction between the n-p dopant pairs, and the non-compensated nature further ensures the creation of the IB. Furthermore, the position and intensity of the IB can be tuned by choosing different combinations and concentrations of the non-compensated n-p pairs. Because of its low cost, chemical

inertness, photo-stability, and excellent charge transport properties¹³, TiO_2 has been considered as one of the most promising candidates for enhanced solar energy utilization, for example as photo-catalysts in hydrogen production via water splitting^{14–16} and as charge collectors in dye-sensitized solar cells^{17,18}.

In this Letter, we propose to develop IBSCs by exploiting the very existence of IBs in non-compensated n-p codoped TiO_2 , and explore theoretically their maximum quantum efficiencies under different design schemes. We first study the quantum efficiency of codoped TiO_2 as ideal IBSCs and show that their maximum efficiency can reach 52.7%. However, a small deviation of the IB position from the optimum value would cause a large drop in the quantum efficiency. To remedy this stringent requirement, we propose a new design scheme where current can also be extracted from the IB, taking advantage of the delocalized nature of the IB built via non-compensated n-p codoping¹⁹. We show that the IB position can now be in a broader range within the intrinsic bandgap for sufficiently high quantum efficiencies, with the maximum efficiency increased to 56.7%. These findings suggest that the second design scheme should be more desirable in facilitating practical implementation of IBSCs.

For convenience, here we reproduce four of the seven ideal conditions of IBSCs² that are specially pertinent to the present work: (C1) full absorption of photons whose energies are sufficient to induce electronic excitations between any two of the three bands; (C2) nonradiative electronic transitions are forbidden; (C3) no current from the IB; (C4) for every range of energies only one of the three absorptions is important (namely, the ranges of energies that induce the three electronic excitations do not overlap with each other). The band diagram and the electron transitions between two of the three bands are shown in Fig. 1. According to C1, C2, and C4, the net electron transitions between two of the three bands per unit time

^{a)}Electronic mail: cuipg@ustc.edu.cn.

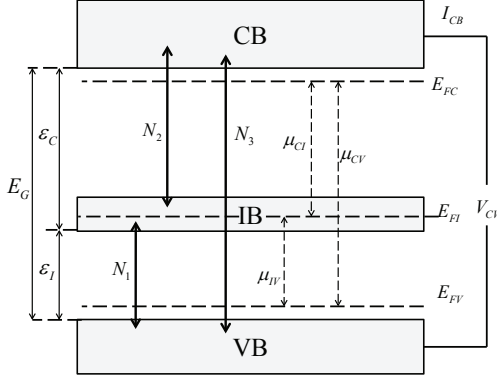


FIG. 1. Band diagram of an intermediate band solar cell. E_G is the intrinsic energy band gap, ε_I is the IB position, and $\varepsilon_C = E_G - \varepsilon_I$ is the IB gap. E_{FV} , E_{FI} and E_{FC} are the quasi-Fermi levels for the three bands. Chemical potentials μ_{IV} , μ_{CV} and μ_{CI} are the spacings between the three quasi-Fermi levels.

and per unit illuminated area are given as:

$$N_1 = \begin{cases} N(\varepsilon_I, \varepsilon_C, T_s, 0) - N(\varepsilon_I, \varepsilon_C, T_a, \mu_{IV}) & \varepsilon_I < E_G/2 \\ N(\varepsilon_I, E_G, T_s, 0) - N(\varepsilon_I, E_G, T_a, \mu_{IV}) & \varepsilon_I \geq E_G/2 \end{cases}$$

$$N_2 = \begin{cases} N(\varepsilon_C, E_G, T_s, 0) - N(\varepsilon_C, E_G, T_a, \mu_{CI}) & \varepsilon_I < E_G/2 \\ N(\varepsilon_C, \varepsilon_I, T_s, 0) - N(\varepsilon_C, \varepsilon_I, T_a, \mu_{CI}) & \varepsilon_I \geq E_G/2 \end{cases}$$

$$N_3 = N(E_G, \infty, T_s, 0) - N(E_G, \infty, T_a, \mu_{CV}). \quad (1)$$

Here E_G is set to 3.2eV for the bandgap of TiO_2 , $T_s = 6000\text{K}$ and $T_a = 300\text{K}$ are the solar temperature and work temperature for the IBSCs, respectively, and the function $N(\varepsilon_m, \varepsilon_M, T, \mu) = \frac{2\pi}{h^3 c^2} \int_{\varepsilon_m}^{\varepsilon_M} \frac{e^2 d\varepsilon}{e^{(\varepsilon - \mu)/kT} - 1}$. On the right hand side of each line of Eq. (1), the first term represents the absorption of photons that generates electron-hole pairs, and the second term the emission of photons that annihilates electron-hole pairs.

If no current outputs from the IB, the number of electrons in the IB should be conserved. When the IB is quite close to the VB, photons that can induce the VB \rightarrow IB transitions are much more than those that can induce the IB \rightarrow CB transitions. As a result, N_1 defined by Eq. (1) is always larger than N_2 if $\varepsilon_I < \varepsilon_1$, as shown in Fig. 2. In contrast, N_1 is always smaller than N_2 if the IB is quite close to the CB ($\varepsilon_I > \varepsilon_4$). The lack of overlap between the ranges of N_1 and N_2 for $\varepsilon_I < \varepsilon_1$ and $\varepsilon_I > \varepsilon_4$ certainly contradicts with the balance of electrons in the IB, indicating that the ideal conditions cannot be satisfied in these cases. For $\varepsilon_I < \varepsilon_1$, the net electron transitions between the VB and IB are suppressed, as they must match the transitions between the IB and CB. The suppression can be caused by several non-ideal factors, such as partial absorption of the photons that induce the VB \rightarrow IB transitions (violation of C1), or nonradiative transitions from the IB to VB (violation of C2). Similarly, for $\varepsilon_I > \varepsilon_4$ electron transitions from the IB to CB

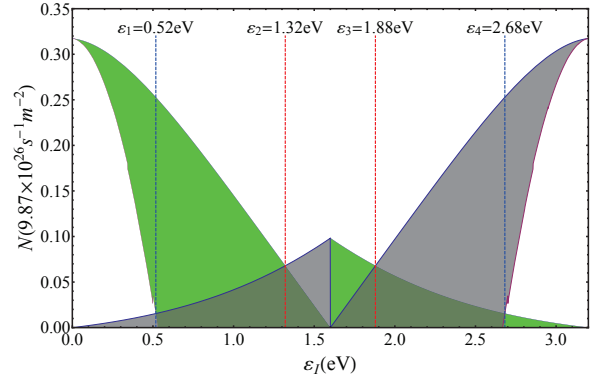


FIG. 2. (Color online) Range of N_1 (green area) and N_2 (gray area) defined in Eq. (1).

are suppressed and the condition C1 cannot be satisfied. For the above two cases, we assume that the smaller one of N_1 and N_2 dominates the two-step transitions from the VB to CB and some non-ideal factors are considered in the other step. For $\varepsilon_1 < \varepsilon_I < \varepsilon_4$, there are overlaps between the ranges of N_1 and N_2 , and the ideal conditions can be satisfied. As a consequence, the current from the CB is obtained as:

$$I_{CB}/q = \begin{cases} N_2 + N_3 & \varepsilon_I < \varepsilon_1 \\ N_2 + N_3, \text{ with } N_1 = N_2 & \varepsilon_1 < \varepsilon_I < \varepsilon_4 \\ N_1 + N_3 & \varepsilon_I > \varepsilon_4 \end{cases} \quad (2)$$

This current is delivered at a voltage $V_{CB} = \mu_{CV}/q$. The quantum efficiency of the IBSCs is given by:

$$\eta = \frac{I_{CB} V_{CB}}{\sigma T_s^4}, \quad (3)$$

where σ is the Stefan-Boltzmann constant.

The optimum quantum efficiency versus the IB position is presented by the black line in Fig. 3. The maximum quantum efficiency, 52.7%, can be obtained given $V_{CB} = 3.00\text{V}$ and $\varepsilon_I = 1.32\text{eV}$ or 1.88eV where N_1 and N_2 are well matched as shown in Fig. 2. The efficiency curve has two symmetrical peaks centered on the mid gap $\varepsilon_I = \varepsilon_C = E_G/2 = 1.6\text{eV}$, a reflection of the particle-hole symmetry in the IB at this location. Since the two peaks are sharp, a small deviation in the IB position from the optimum value would lead to a large drop in the quantum efficiency. This large drop could be partly responsible for the observation that the potential high efficiency of IBSCs has not been achieved experimentally, i. e. the IB would have to be built exactly at the optimum position.

To relax this stringent working condition for IBs, we explore a new design scheme by extracting current also from the IB. N_1 can be much larger than N_2 when $\varepsilon_I < 1.32\text{eV}$ (Fig. 2). However, if there is no current from the IB, the large value of N_1 cannot be fully exploited. Extracting current from the IB can make a better use of the possible high value of N_1 , thus improving the efficiency.

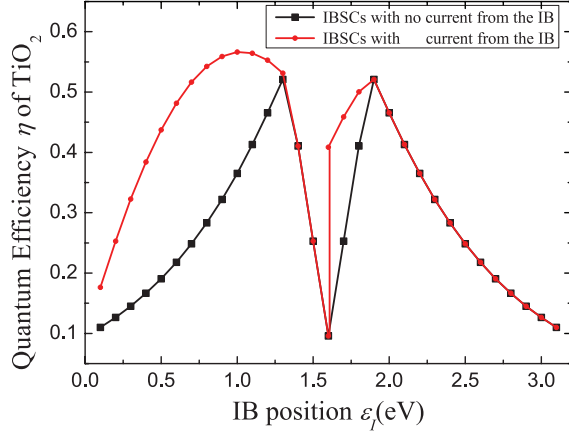


FIG. 3. (Color online) The optimum quantum efficiency of TiO_2 as IBSCs without (black line) and with (red line) current from the IB versus the IB position.

In this scheme, the IB should be connected to a charge collecting contact that must be isolated from that of the CB. Here we note that in the recent experimental study of the effect of charge transport in the IB on the efficiency, both the IB and CB were connected to the same charge collecting contact⁵.

We assume that the net electron transitions between two of the three bands are still determined by Eq. (1). As the IB is not an electron reservoir, only electrons can be extracted from the IB. The currents from the IB and the CB are given respectively by:

$$\begin{aligned} I_{IB}/q &= N_1 - N_2 \geq 0, \\ I_{CB}/q &= N_2 + N_3. \end{aligned} \quad (4)$$

I_{IB} and I_{CB} are delivered at two different voltages, $V_{IB} = \mu_{IV}/q$ and $V_{CB} = \mu_{CV}/q$. The quantum efficiency in this new scheme is revised as:

$$\eta = \frac{I_{IB}V_{IB} + I_{CB}V_{CB}}{\sigma T_s^4} \quad (5)$$

In Fig. 3, the red line represents the optimum quantum efficiency of TiO_2 -based IBSCs versus the IB position, with current extracted from the IB. The maximum quantum efficiency can reach 56.7% with $\varepsilon_I = 1.03\text{eV}$, $V_{CB} = 3.00\text{V}$ and $V_{IB} = 0.97\text{V}$. It also exhibits the obvious double-peaked feature, but the two peaks are no longer symmetric, since the IB can only outputs electrons. Most notably, in the vicinity of $\varepsilon_I = 1.03\text{eV}$, the efficiency within the present design scheme can be substantially higher than that of the ideal one, and the stringent requirement of the IB position is relaxed. When the IB is quite close to the CB, e.g. $\varepsilon_I > 1.88\text{eV}$, photons that can induce the $\text{IB} \rightarrow \text{CB}$ transitions are abundant, and all the electrons excited to the IB from VB can be readily excited to the CB; therefore, there is no need to extract current from the IB in this regime (see Fig. 3). The jump in the quantum efficiency at the mid gap ($\varepsilon_I = \varepsilon_C = E_G/2 =$

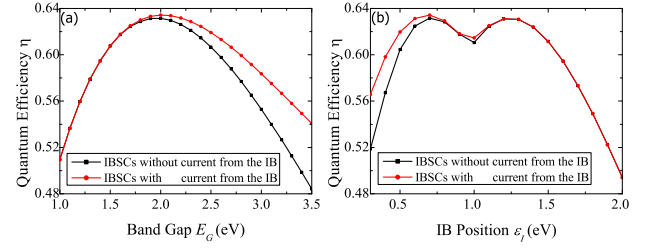


FIG. 4. (Color online) The optimum quantum efficiency of general IBSCs without (black line) and with (red line) current from the IB versus (a) the band gap and (b) IB position.

1.6eV) is due to the assumed condition C4. If the overlap between the three absorption coefficients^{20,21} is considered, the jump, or discontinuity, can be removed, with the main results staying valid.

Here we also briefly look into the efficiency improvement for other materials as IBSCs with current extraction from the IBs. Fig. 4(a) shows the optimum quantum efficiency of general IBSCs without and with current from the IB versus the band gap. The maximum efficiency of the IBSCs under the new design scheme can reach 63.4% with $E_G = 2.02\text{eV}$ and $\varepsilon_I = 0.69\text{eV}$, which is only slightly higher than the maximum efficiency of 63.2% without current from the IB. However, as shown in Fig. 4(a), extracting current from the IB can significantly improve the efficiency for wide bandgap materials ($E_G > 2\text{eV}$), suggesting that the present new design scheme is more promising for oxide-based IBSCs. The optimum efficiency of general IBSCs versus the IB position is shown in Fig. 4(b), which also exhibits the double-peaked feature. In agreement with the results for TiO_2 , there is also no need to extract current from the IB of general IBSCs when the IB is close to the CB.

In summary, we have explored the optimum quantum efficiency of IBSCs based on codoped TiO_2 under two different design schemes. When the ideal conditions are preserved, the corresponding maximum quantum efficiency for the codoped TiO_2 can reach 52.7% but requires a stringent IB position. Upon extracting current from the IB, the IB position can be in a wide range, with a maximum efficiency of 56.7%. These results should facilitate experimental realization of IBSCs, and make n-p codoped TiO_2 as appealing candidate materials for high-efficiency solar energy utilization.

Acknowledgements: This work was supported by the National Natural Science Foundation of China under Grant No. 11034006 and in part by Division of Materials Sciences and Engineering, Basic Energy Sciences, US Department of Energy. We thank Tianli Feng, Guangwei Deng, and Yi Xia for valuable discussions.

¹W. Gutera, *et al.*, Appl. Phys. Lett. **94**, 223504 (2009).

²A. Luque and A. Marti, Phys. Rev. Lett. **78**, 5014 (1997).

³W. Shockley and H. J. Queisser, J. Appl. Phys. **32**, 510(1961).

⁴A. Marti, *et al.*, Phys. Rev. Lett. **97**, 247701 (2006).

⁵N. López, *et al.*, Phys. Rev. Lett. **106**, 028701 (2011).

⁶A. Luque, *et al.*, Appl. Phys. Lett. **87**, 083505 (2005).

- ⁷A. Luque and A. Marti, Adv. Mater. **22**, 160 (2010).
- ⁸R. W. Peng, M. Mazzer, and K. W. J. Barnham, Appl. Phys. Lett. **83**, 770 (2003).
- ⁹V. Popescu, *et al.*, Phys. Rev. B **78**, 205321 (2008).
- ¹⁰W. M. Wang, A. S. Lin, and J. D. Phillips, Appl. Phys. Lett. **95**, 011103 (2009).
- ¹¹B. Lee and L. W. Wang, Appl. Phys. Lett. **96**, 071903 (2010).
- ¹²W. G. Zhu, *et al.*, Phys. Rev. Lett. **103**, 226401 (2009).
- ¹³A. Fujishima, X. T. Zhang, and D. A. Tryk, Surf. Sci. Rep. **63**, 515 (2008).
- ¹⁴A. Fujishima and K. Honda, Nature **238**, 37(1972).
- ¹⁵R. Asahi, *et al.*, Science **293**, 269 (2001).
- ¹⁶S. U. M. Khan, M. Al-Shahry, and W. B. Ingler Jr., Science **297**, 2243 (2002).
- ¹⁷B. O'Regan and M. Gratzel, Nature **353**, 737 (1991).
- ¹⁸U. Bach, *et al.*, Nature **395**, 583 (1998).
- ¹⁹N. Mannella, *et al.*, to be published.
- ²⁰L. Cuadra, A. Mart, and A. Luque, IEEE Trans. Electron Devices **51**, 1002 (2004).
- ²¹T.S. Navruz and M. Saritas, Solar Energy Materials & Solar Cells **92**, 273 (2008).